論文 / 著書情報
Article / Book Information

論題(和文)	
Title(English)	Wind Force Estimation on a Nonlinear Equivalent SDOF Model by Equivalent-Input-Disturbance (EID) Method
著者(和文)	SORIANO Razelle Dennise A., 佐藤大樹, 宮本皓, 陳引力, 余錦華
Authors(English)	SORIANO Razelle Dennise A., SATO Daiki, Kou Miyamoto, Yinli Chen, Jinhua She
出典 / Citation	日本建築学会関東支部研究報告集, Ⅰ, , pp. 461-464
Citation(English)	, Ⅰ, , pp. 461-464
発行日 / Pub. date	2024, 3
権利情報	一般社団法人 日本建築学会

2023年度日本建築学会
関東支部研究報告集 I
2024年3月

Wind Force Estimation on a Nonlinear Equivalent SDOF Model by Equivalent-Input-Disturbance (EID) Method

構造ー振動　　正会員 ○ SORIANO Razelle Dennise A.*1　同 佐藤 大樹*2
同 宮本 皓*3　同 陳 引力*4
同 佘 錦華*5

Wind force estimation, Equivalent SDOF, EID method, Base-isolation, Nonlinear system

1. INTRODUCTION

1.1. Background

Seismic base-isolation is widely recognized for its effectiveness in reducing earthquake damage, particularly in low- and medium-rise structures. However, the system's implementation in high-rise buildings has already been gaining attention, with numerous tall buildings incorporating base-isolation systems in the past few decades [1].

As the structure's height increases, it becomes more susceptible to extreme wind forces, making wind load analysis an integral factor in the design process. The existing design guidelines for wind-induced response of seismically base-isolated buildings are established but are limited only to the elastic range of the isolation system. Yet taller base-isolated structures exposed to stronger winds pose a risk of the structural elements of the isolation layer exceeding the system's elastic limits. If this is the case, the elasto-plastic characteristics of the isolation system must be considered, and this can be done by evaluating the wind-induced response of the structure by time-history analysis [2].

Time-history analysis requires the use of actual wind forces acting on the structure. These wind forces are currently derived from wind tunnel experiments and numerical methods which are limited in producing an accurate model that correctly depicts certain field conditions such as incident turbulence and the characteristics of the surrounding terrain. Hence, verification of the accuracy of the wind forces obtained from these methods is necessary. One way to do this is by calculating the wind forces from wind-induced responses recorded from monitoring systems.

Miyamoto et al. used a method called the Equivalent-Input-Disturbance (EID) approach to estimate the wind loads of a seismically base-isolated building using only the velocity responses [3]. However, the nonlinearity of the said structure has not been considered. Therefore, this study aims to use the EID method to estimate the wind forces acting on a base-isolated tall building, simplified as a single degree of freedom (SDOF) model, considering two scenarios: the isolation layer having a linear and nonlinear hysteretic damper.

2. THEORETICAL BACKGROUND

2.1. Equivalent SDOF Model

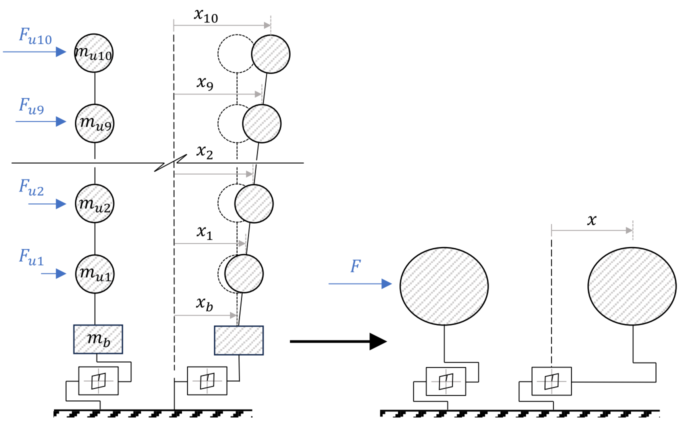

Figure 1. Concept of equivalent SDOF model

The estimation of wind forces on a nonlinear tall seismically isolated building using only velocity responses by EID method have not been investigated yet. As a first step towards this goal, a seismically isolated building given by an 11-DOF lumped mass model is simplified into an equivalent SDOF model assuming that the upper structure remains linear and elastic and moves as a rigid body relying on the flexibility of the isolation system [4]. The concept of this assumption is shown in Figure 1. The properties of the equivalent SDOF model, hereafter referred to simply as the SDOF model, are calculated using the following relationships [5]:

$$m = m_b + \sum_{i=1}^{10} m_{ui} \quad (1)$$

$$k_1 = k_{be} \quad (2a)$$

$$k_2 = k_{bp} \quad (2b)$$

$$Q_y = Q_{by} \quad (3)$$

$$x_y = x_{by} \quad (4)$$

$$\zeta = \zeta_b \quad (5)$$

$$F(t) = \sum_{i=1}^{10} F_{ui} \quad (6)$$

Wind Force Estimation on a Nonlinear Equivalent SDOF model using the EID Approach

SORIANO, Razelle Dennise A., SATO, Daiki, MIYAMOTO, Kou, CHEN, Yinli, SHE, Jinhua where m, k_1, k_2, Q_y, x_y, ζ and $F(t)$ are the mass, initial stiffness, post-yield stiffness, yield shear force, yield displacement, damping ratio and wind force of the SDOF model, respectively. The mass of the isolation layer and the ith story of the upper structure are given by m_b and m_{ui}, respectively. The variables k_{be}, k_{bp}, Q_{by}, x_{by}, and ζ_b are the initial stiffness, post-yield stiffness, yield shear force, yield displacement and damping ratio of the isolation layer having bilinear behavior. The ith story of the 11-DOF model is subjected to the wind force F_{ui}. The properties of the 11-DOF model are shown in Table 1. The wind forces used in the analysis were derived from a wind-tunnel experiment [6] with a 500-year return period in the along-wind direction and a design wind velocity of 63.8 m/s.

Table 1. Properties of the 11-DOF model

	Upper structure	Isolation layer
Natural period	T_u = 2.0 s	T_0 = 4.0 s
Density	ρ_u = 180 kg/m^3	ρ_0 = 3644 kg/m^2
Height	H = 100 m	
Area	A = 625 m^2	A = 625 m^2
Damping ratio	ζ_u = 2.0%	ζ_b = 0%
Yield shear coeff.		α_{by} = 0.03
Yield deformation		x_{by} = 1 cm

2.2. Wind Force Estimation by EID Method

This section discusses the estimation of wind forces using the EID method [3]. The equation of motion of an SDOF model subjected to external wind forces:

$$m\ddot{x}(t) + c\dot{x}(t) + kx(t) = E_d F(t) + E_u u(t)m \qquad (7)$$

where $\{\ddot{x}(t)\}$, $\{\dot{x}(t)\}$ and $\{x(t)\}$ are the dynamic responses of the model, namely, acceleration, velocity, and displacement vectors, respectively. Also, m, c and k are the property matrices, namely, mass, damping and stiffness, respectively. E_d is the input channel of the wind force $F(t)$ and $u(t)$ and E_u are the control input and control-input channel, respectively. The system does not have an active control, but a virtual active control is employed to apply EID approach to estimate the wind forces. The state space representation of the system is given by:

$$\dot{z}(t) = Az(t) + B_d d(t) + B_u u(t) \qquad (8)$$

$$y(t) = Cz(t) \qquad (9)$$

where

$$\begin{cases} A = \begin{bmatrix} 0 & 1 \\ -k/m & -c/m \end{bmatrix} & B_d = \begin{bmatrix} 0 \\ -E_d/m \end{bmatrix} \\ B_u = \begin{bmatrix} 0 \\ E_u \end{bmatrix} & z(t) = \begin{bmatrix} x(t) \\ \dot{x}(t) \end{bmatrix} \\ d(t) = F(t) & \end{cases} \qquad (10)$$

where A is the system matrix, B_d is the disturbance input matrix, B_u is the control input matrix, $d(t)$ is the disturbance on the system (e.g., wind force) and $z(t)$ is the state of the system. The output, $y(t)$ is given by the output matrix, C that indicates the placement of the sensors. In this paper, it is assumed that only the velocity responses are recorded by the sensors. Thus, $C = [0, 1]$ so that $y(t)$ only yields the value of the velocity responses.

The block diagram of Eqs. (8) and (9) is shown in Figure 2(a) whereas Figure 2(b) shows the system with an EID, $d_e(t)$, with and output $\bar{y}(t)$. Note that in this paper, the model does not have an active control $u(t) = 0$. Instead, we use the control input channel to apply the EID approach, assuming $B_u = B_d$. If $y(t) = \bar{y}(t)$, it follows that $d_e(t)$ = original disturbance $d(t)$.

The full state observer of Eq. (8) is given by:

$$\begin{cases} \dot{\hat{z}}(t) = A\hat{z}(t) + LC\,[z(t) - \hat{z}(t)] \\ \hat{y}(t) = C\hat{z}(t) \end{cases} \qquad (11)$$

where $\hat{z}(t)$ is an estimated $z(t)$ and L is the observer gain. Combining Eq. (8) and (11) yields:

$$\Delta\dot{z}(t) = (A - LC)\Delta z(t) + B_d d(t) \qquad (12)$$

where $\Delta z(t)$ is the difference between $z(t)$ and $\hat{z}(t)$. Since the system is considered to be controllable, there exist a signal $\Delta d(t)$ that satisfies the following:

$$\Delta\dot{z}(t) = A\Delta z(t) + B_d \Delta d(t) \qquad (13)$$

Equating Eqs. (12) and (13) yields the value for the estimated wind load, $\hat{d}_e(t)$:

$$\begin{cases} \hat{d}_e(t) = {B_d}^{+} LC\Delta z(t) \\ \hat{d}_e(t) = d_e(t) - \Delta d(t) \end{cases} \qquad (14)$$

where ${B_d}^{+}$ is the pseudo inverse matrix of B_d given by the following equation.

$${B_d}^{+} = \left({B_d}^T B_d\right)^{-1} {B_d}^T \qquad (15)$$

2.3. Design of Observer Gain

The observer gain, L in the EID estimation is obtained using the Linear Quadratic Regulator (LQR) design. LQR is considered as an optimal control in which the quadratic performance index (cost function), J is minimized.

$$J = \int_0^{\infty} \{z^T(t)\boldsymbol{Q}x(t) + u^T(t)\boldsymbol{R}u(t)\}dt \qquad (16)$$

where $\boldsymbol{Q}$ and $\boldsymbol{R}$ are the weighing matrices of the state, z(t) and the control, $u(t)$, respectively. The matrix $\boldsymbol{Q}$ is a positive semi-definite and $\boldsymbol{R}$ is a positive definite. These two matrices are often diagonal, and the diagonal elements are adjusted to adjust the weights of either the state or the control [7]. The LQR control law,

$$u = -Lz \quad (17)$$

is designed to minimize $J = \lim_{t \to \infty} J(t)$. Since J is quadratic, there exists a solution for the observer gain L, given by

$$L = -\boldsymbol{R}^{-1} C^T P \quad (18)$$

where P is the solution to the algebraic Ricatti equation:

$$A^T P + AP - PC\boldsymbol{R}^{-1} C^T P + \boldsymbol{Q} = 0 \quad (19)$$

$$\boldsymbol{Q} = [Q_1 \quad Q_2] \quad (20) \qquad\qquad \boldsymbol{R} = [R_c] \quad (21)$$

In this study, there are no displacement response and control input to be optimized. Thus, $Q_1 = 10^0$ and $R_c = 10^0$ and different values of Q_2 are investigated, namely, 10^8, 10^{10} and 10^{16}, referred to as "low", "mid" and "high", respectively.

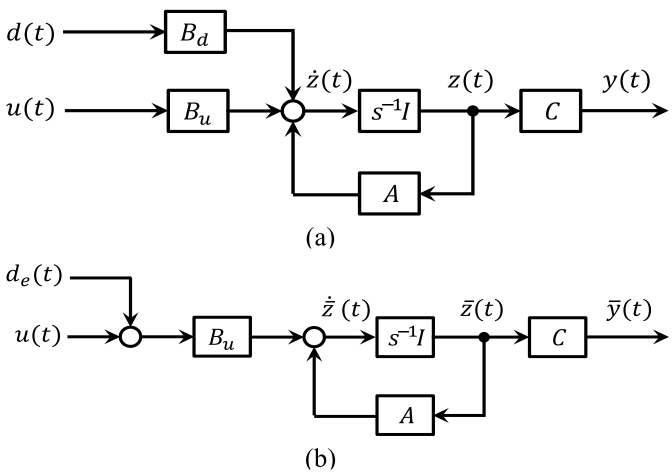

Figure 2. Concept of EID [3].

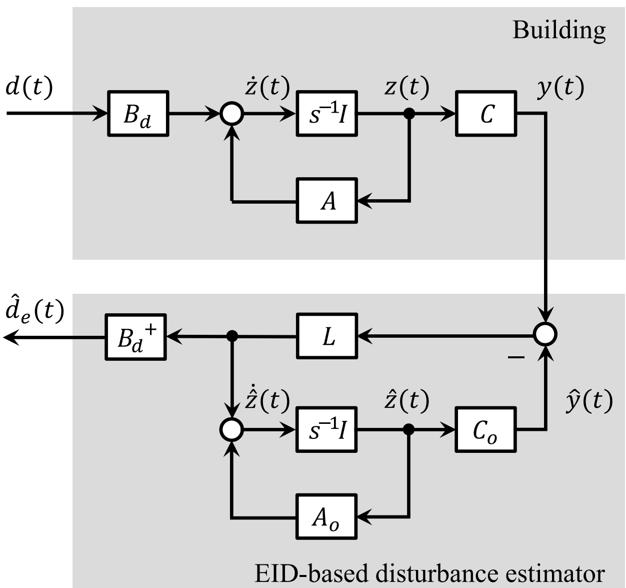

Figure 3. EID block diagram for disturbance estimation

4. RESULTS

4.1. Linear model

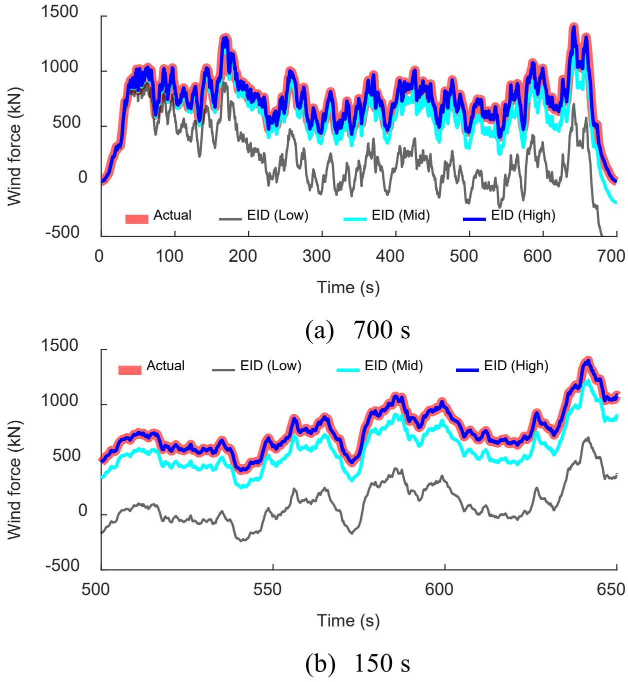

Figure 4. Estimated wind force time-history – linear model.

In this section, the wind forces acting on the equivalent SDOF model with linear hysteretic dampers are estimated by calculating the equivalent disturbance, $\widehat{d_e}(t)$ shown in the block diagram in Figure 3. Different values of observer gain, L, are used. Shown in Figure 4 are the time-histories of the actual and the estimated wind forces for different observer gain values. It can be seen that for a low and mid observer gain value, the error accumulates for each time step leading to an inaccurate estimate at longer time values. On the other hand, wind force estimates using high observer gain values are accurate throughout the time duration.

4.2. Nonlinear model

In this section, the wind forces acting on the equivalent SDOF model with hysteretic dampers behaving bilinearly are estimated by using the block diagram shown in Figure 5. Since the stiffness of the system changes with time, the restoring force, $F_h(t)$ is calculated separately per time step [8]. Similar to the previous section, the equivalent disturbance, $\widehat{d_e}(t)$ gives the wind force estimate by EID method.
The results of the wind force estimation for the nonlinear model are shown in Figure (6). It can be seen in the figure that unlike the linear case, for low and mid values of observer gain, the wind force estimates are inaccurate only on certain time durations, particularly during the time that the hysteretic damper starts yielding ($t \approx 100$ to 300 s). This inaccuracy eventually decreases as the observer gain tries to optimize the response estimates. This shows that when the observer gain is not optimized, nonlinearity affects the performance of wind force estimation. Also, another factor that might be affecting the accuracy of the estimates during the time of yielding is

the use of LQR for the estimation of the observer gain. However, for the optimized or high observer gain values, accurate estimates of the wind forces are obtained throughout the time duration.

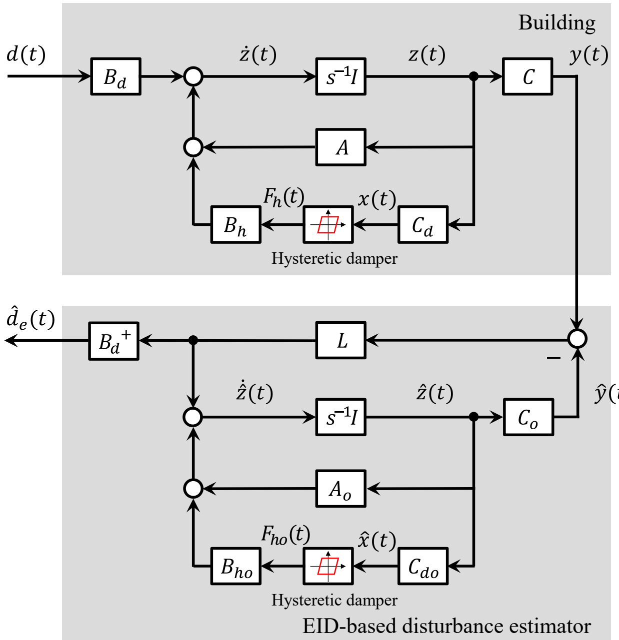

Figure 5. EID block diagram for nonlinear model

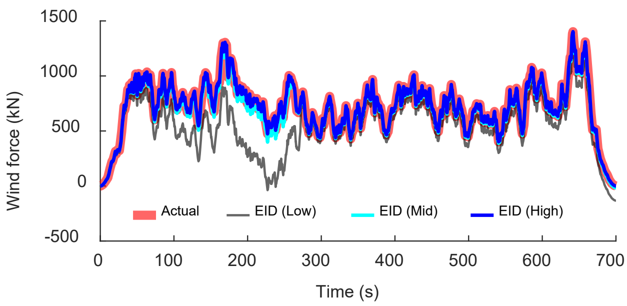

(a) 700 s

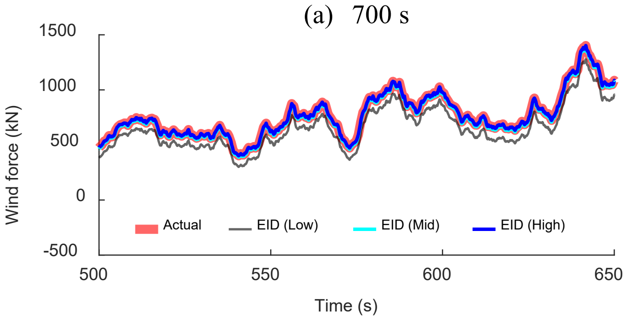

(b) 150 s

Figure 6. Estimated wind force time-history – nonlinear model.

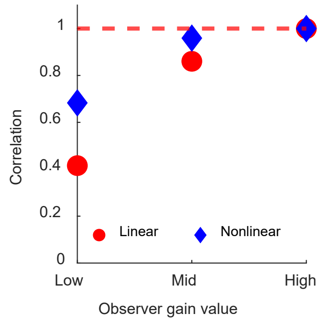

Figure 7. Correlation of wind forces for the linear and nonlinear models.

Also shown in Figure 7 is the comparison of the correlation coefficient of the estimated wind forces for both the linear and nonlinear models. It can be seen here that in both cases, the wind forces are estimated with very high accuracy when the value of the observer gain is high. In contrast, the nonlinear model obtained more accurate wind force estimates for the low and mid observer gain values.

5. CONCLUSION

In this paper, the wind forces acting on an 11-DOF base-isolated building, modeled as an equivalent SDOF system was estimated using the EID method. The estimation was done under the assumption that only the velocity responses are available. The accuracy of the estimation method was tested for models with linear and nonlinear hysteretic dampers and different values of observer gains were used. The results showed that the EID method with a high value of observer gain can estimate the wind forces accurately for both models with linear and nonlinear hysteretic dampers.

REFERENCES

[1] Ma, C. F., Zhang, Y. H., Tan, P., & Zhou, F. L. (2014). Seismic response of base-isolated high-rise buildings under fully nonstationary excitation. *Shock and Vibration*, *2014*, 1-11.

[2] Japan Society of Seismic Isolation (2018), JSSI Guideline for Wind-resistant Design of Seismically Base-Isolated Buildings (in English)

[3] Miyamoto, K., Sato, D., She, J., Chen, Y., & Nakano, S. (2022, July). Wind-load estimation with equivalent-input-disturbance approach. In *2022 IEEE/ASME International Conference on Advanced Intelligent Mechatronics (AIM)* (pp. 921-925). IEEE.

[4] Liu, T., Zordan, T., Briseghella, B., & Zhang, Q. (2014). Evaluation of equivalent linearization analysis methods for seismically isolated buildings characterized by SDOF systems. *Engineering Structures*, *59*, 619-634

[5] 銭暁鑫, & 佐藤. (2023). 高層免震建物の風応答時における鋼材ダンパーの吸収エネルギー評価のための等価 1 質点系モデル. *日本建築学会大会学術講演梗概集*, 607-608.

[6] Marukawa, H., Ookuma, T., Kitamura, H., Yoshie, K., Tsurumi, S., & Sato, D. (2010). Nergy input of local wind forces for high-rise buildings based on wind tunnel test-Part2 local wind force characteristics of rectangular high-rise buildings. In *AIJ annual conference in Hokuriku* (pp. 193-194).

[7] Brunton, S. L., & Kutz, J. N. (2022). Data-driven science and engineering: Machine learning, dynamical systems, and control. Cambridge University Press.

[8] Chen, Y., Sato, D., Miyamoto, K., & She, J. (2022). Response-spectrum-based design method for active base-isolated buildings with viscous dampers and hysteretic dampers. *Mechanical Systems and Signal*

*1 東京工業大学 大学院生
*2 東京工業大学 准教授・博士（工学）
*3 清水建築 技術研究所・博士（工学）
*4 東京理科大学 助教・博士（学術）
*5 東京工科大学 教授・博士（工学）

* Graduate Student, Tokyo Institute of Technology *1
* Associate Professor, Tokyo Institute of Technology, Dr. Eng.*2
* Researcher, Institute of Technology, Shimizu Corporation, Dr. Eng.*3
* Assistant Professor, Dept. of Arch., Tokyo Univ. of Science, Ph.D.*4
* Professor, Dept. of Mech. Eng., Tokyo Univ. of Technology, Dr. Eng.*5